

Diatom demography in winter – simulated by the Lagrangian Ensemble method

JOHN WOODS,¹ AND
WOLFGANG BARKMANN²

¹NERC Oceanography Unit, Physics Department, Oxford University, Parks Rd., Oxford OX1 3DU, United Kingdom

²Oceanography Department, University of Southampton, Highfield, Southampton SO9 5NH, United Kingdom

ABSTRACT

According to Sverdrup's (1953) model of the spring bloom, phytoplankton biomass decreases in winter when the mixed layer depth exceeds the critical depth. We have used a one-dimensional mathematical model integrated by the Lagrangian Ensemble method to simulate a population of diatoms during the winter between two growing seasons off the Azores. The model allows us to diagnose the demographic changes in the simulated diatom population from a variety of perspectives. The total population falls to a minimum of 70 million diatoms m^{-2} at the end of February. The vertical distribution of the population dynamics is first analysed in terms of daily Eulerian averages over 1 m depth intervals. Growth starts in February when the diurnal thermocline becomes shallower than 50 m, but while the mixed layer is still 200 m deep. The natural mortality has a minimum in winter because it is reduced (in the model) with temperature and population density. Eulerian analysis suggests that in winter, diatoms have a life expectancy of more than 3 months, so a significant number will survive the months of December, January and February when there is very little growth. Losses to grazing are negligible in winter. Lagrangian analysis shows how an individual diatom responds to its changing ambient environment caused by variation in depth (due to turbulent mixing) and the diurnal and seasonal changes in the photosynthetically active radiance. The different trajectories followed by the thousands of plankton particles simulated by the model produce diversity in growth rate ranging over several orders of magnitude, so care has to be taken in statistical analysis.

The paper ends with a re-assessment of the value of the critical depth and compensation depth as predictors for onset of the spring bloom. The compensation depth was computed by Eulerian averaging over 1 m depth intervals each day. For 1 month after the vernal equinox the compensation depth follows the ascent of the mixed layer as it rises from a depth of 100 m to 40 m. Lagrangian analysis reveals that this is due to the photo-adaptation better matching the ambient irradiance experienced by diatoms in the mixed layer compared with those at the same depth in the seasonal thermocline. By mid-April the spring bloom has already advanced so far that self shading influences the compensation depth, which then rises into the mixed layer. We conclude that Sverdrup's criterion is not useful for predicting changes in the diatom population simulated by our model.

Key words: diatoms, Azores, overwintering, model, mixed layer depth, compensation depth, critical depth, Lagrangian analysis, Eulerian analysis

INTRODUCTION

This paper addresses the following scientific problem: what factors determine the winter survival of phytoplankton in the open ocean? Specifically we want to know whether a one-dimensional model based on relatively simple assumptions about plankton growth and behaviour and driven by climatology is capable of simulating a population of diatoms that survives the winter without introducing unrealistic algorithms or tuning the model.

There have been very few theoretical investigations of the survival of plankton populations in winter. Interest has focused more on the conditions for the spring bloom (Riley, 1942; Sverdrup, 1953; Marra and Ho, 1993; Taylor and Stephens, 1993). Sverdrup's (1953) classic model predicted that phytoplankton biomass decreases in winter when the mixed layer depth exceeds the critical depth. The problem of winter survival is important to modellers seeking to integrate their models for several years. For example, Woods and Barkmann (1993) found that the respiration rate that gives realistic simulation of summer conditions is too high in winter, and reduced it with temperature and

Received for publication 21 July 1993

Accepted for publication 4 August 1993

©1993 Blackwell Scientific Publications, Inc.

with population density following a similar approach used by Fasham (1993) to deal with inadequate grazing in winter.

There are remarkably few empirical descriptions of the winter changes in plankton population. Colebrook (1979, 1985, 1986) has discussed the importance of winter conditions to explain the seasonal and inter-annual variations of phytoplankton biomass measured by continuous plankton recorder. Corlett (1953) described the seasonal variation of the number of diatoms in the water column at Ocean Weather Station "I". Cushing (1975) has discussed the seasonal cycle of phytoplankton in the Atlantic in terms of chlorophyll concentration and cell numbers. Dickey *et al.* (1991) report the results of measurements from March to May inclusive in the Sargasso Sea made as part of the Biowatt program.

There is a substantial literature on the biological response of phytoplankton to winter conditions (Raymont, 1980). Changes in physiology and behaviour of plankton deduced from a combination of sampling at sea and experiments in the laboratory indicate a variety of strategies available for coping with the inclement winter environment (Margelef, 1978). The first steps have been taken to incorporate these findings into model equations, starting with physiological response to the physical environment which may have general applicability. For example, it is now common to model respiration as a function of temperature and light, and some attention is being paid to the role of turbulence in zooplankton behaviour. However, it is not yet possible to take account of changes in the properties of particular species; models designed to simulate the upper ocean ecosystem tend to include only one guild (functional group) per trophic level. Primary production is often represented by a single guild of phytoplankton with attributes reminiscent of diatoms, and secondary production by a single guild reminiscent of copepods like *Calanus*. Until the next generation of models, with several guilds per trophic level, becomes available it is premature to incorporate more detailed representation of stages in biological growth.

Meanwhile we can make a start by asking whether the present generation of models can successfully simulate plankton survival in winter without invoking seasonal changes in the rules governing plankton physiology and behaviour. Before including biological changes into the models it is desirable to develop a detailed understanding of the nature of the physical environment in the upper ocean during winter and the impact it has on plankton constrained to the simplified rules of growth and behaviour found in contemporary models. That will have value in its own right and it will provide a

benchmark against which to assess the results of future studies that incorporate more realistic biology.

In such investigations the Lagrangian Ensemble (LE) method of integrating plankton models offers advantages over the classical Eulerian Continuum models. By simulating the growth and behaviour of the plankton community in terms of an ensemble of families* it is possible to introduce the biological rules in a more realistic manner. The LE method is well suited to demographic studies of plankton populations: the simulated distributions can be diagnosed in terms of population statistics and audit trails of individual particles. Our study involved integration of the model under conditions of astronomical and climatological forcing encountered off the Azores (41°N, 27°W).

THE MODEL

The LE'93 model used in this investigation has been described elsewhere (Woods and Barkmann, 1993). Equations and constants are summarized in the Appendix (Section 1). The model contains the minimum portfolio of variables needed to simulate the upper ocean ecosystem (Table 1); the model equations describe the interactions between the variables.

Integration

The model was initialized in winter with a 200 m deep mixed layer charged with nitrate (4 mmol nitrogen m^{-3}) but with no ammonium. The initial population of 50 million diatoms was distributed between 4000 families in the mixed layer which automatically split in the first time step to give 7000 families, which declined (by natural mortality) to a minimum of 800 in summer and

Table 1. Variables in the model.

Environment	Variable
Physical	Light (27 spectral bands), turbulence, temperature
Chemical	
Dissolved	Nitrate, ammonium, inorganic carbon
Particulate	Detritus (dead plankton), faecal pellets
Biological	
Explicit	Phytoplankton (diatoms), herbivores (copepods)
Implicit	Carnivores, bacteria

*Families contain many diatoms following the same trajectory, as though they are contained within a particle which behaves like a single plankter.

then increased by splitting next autumn. (The process of splitting will be discussed later.)

The model was integrated for 2 y in half-hour time steps, in response to (1) astronomical variation in solar elevation and (2) variation of cloud cover and surface atmospheric fluxes interpolated between Bunker's monthly mean climatology (Isemer and Hasse, 1986), at two fixed locations (a) off the Azores (41°N, 27°W) and (b) south of Greenland (55°N, 37°W). The model does not simulate the effects of varying weather, so we can only discuss the average cycle of events each year rather than the particular events in any given year, but that does not invalidate the use of the model to illustrate winter survival. Indeed the diatoms that do survive live for several weeks, so short-term fluctuations in the weather are of less concern than the seasonal trend, which is adequately captured by the monthly mean atmospheric data. We could have forced the model by using the actual sequence of monthly mean atmospheric data in a particular year (Taylor and Stephens, 1993). However, we consider it of little value to attempt to simulate events encountered at sea unless account is taken not only of the impact of transient weather systems in the atmosphere, but also of those inside the ocean (Strass, 1992) which have time scales better matched to the life expectancy of particles surviving in winter.

Output

The ecosystem simulated by the model was recorded in three databases. The Eulerian database records time series of vertical profiles of environmental variables (Table 1). The Lagrangian database records the life histories of every family of identically adapted diatoms. The register records the depth and time of every family event occurring in the water column, including cell divisions, deaths and splits.

Those three data sets document the changes that occurred in the simulated ecosystem. The Eulerian database contains all the information produced by classical models, with the profiles of biological variables derived in this case from statistical analysis of the ensemble of families in each 1 m thick layer. The Lagrangian database supports diagnosis of changes in the ecosystem by providing audit trails of the development of each of the families involved in a particular development. The register is used to calculate statistics of the whole community, such as seasonal changes in birth rate and life expectancy.

THE LAGRANGIAN VIEW

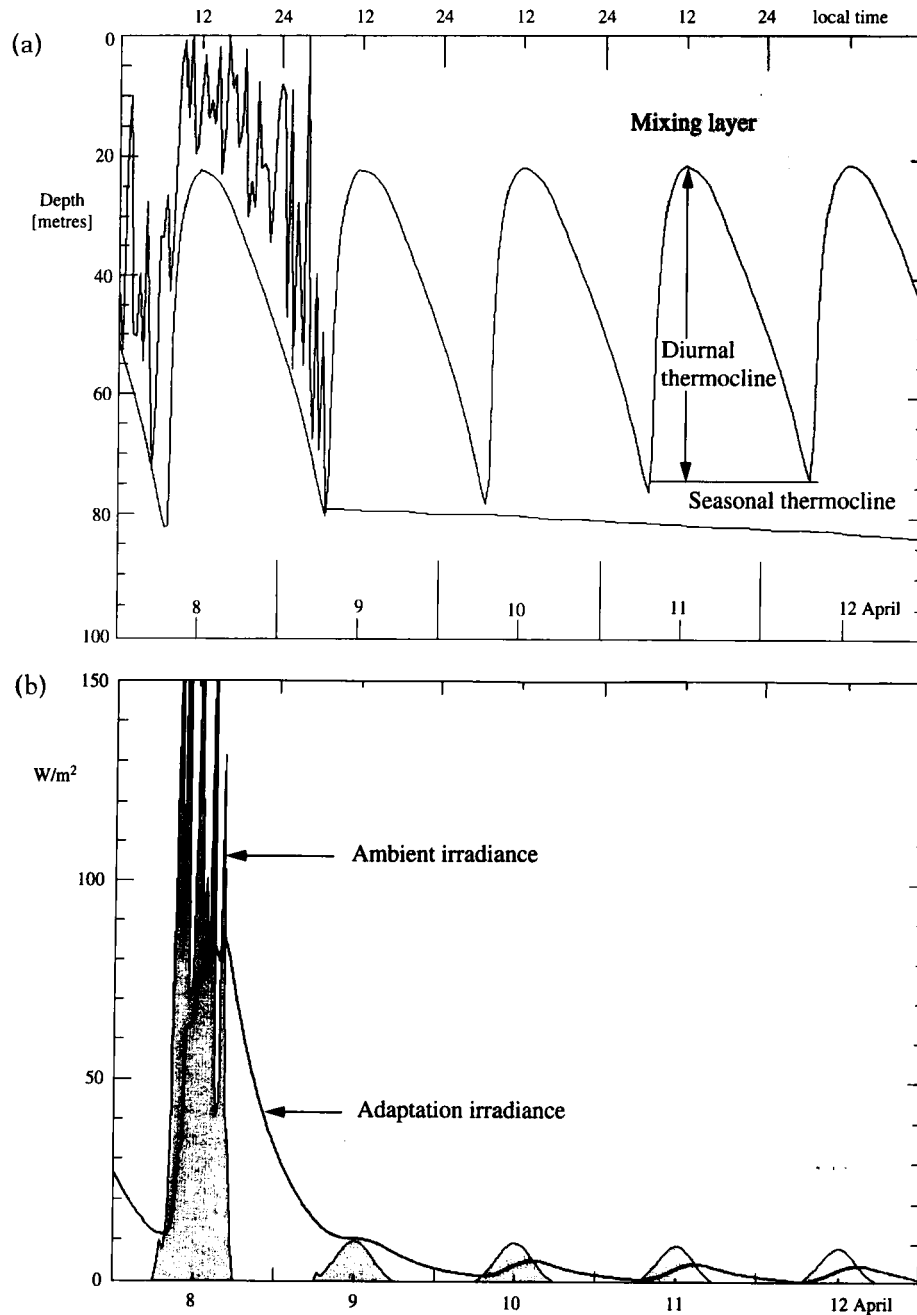
The model represents the phytoplankton in terms of an ensemble of families, each of which contains a number

of identical diatoms. That number can increase by cell division, an event that involves every member, and it can decrease as the result of grazing (which we shall show is negligible in winter). Each family is given a numerical label, which allows us to extract an audit trail showing the ambient environment it experiences at any stage in its history, and its response to that environment. The ambient environment of a family is defined as the set of values of all environmental fields at its location at one time step in the integration. Figure 1 shows the audit trail for one family (number 83002) from 8 to 12 April.

Each family follows a unique trajectory. Its depth is changed by motion of the water, and by its own motion through the water. In this model the only water motion that matters is the turbulence in the mixing layer; at each time step, a particle in the mixing layer is displaced randomly to a new depth between the surface and the turbocline at the base of the mixing layer. The water below the turbocline is assumed to be in laminar flow (Woods, 1968). Solar heating causes the turbocline to rise in the day, leaving most of the diatom families in laminar flow during the hours when they are exposed to sunlight (Woods and Onken, 1982). However, some remain in the mixing layer during the day and experience a random variation in ambient irradiance commensurate with the changes in their depth induced by turbulent mixing. Figure 1(a) shows the trajectory of family 83002, which passes the daylight hours of 8 April in the mixing layer and is subducted next morning at a depth of 80 m into the thermocline where it remains sinking slowly through the water at terminal speed (1 m d^{-1}).

The diatoms in a family share a common energy pool, which increases during the day by photosynthesis at a rate that depends on the ambient irradiance at each time step, and on the irradiance value to which the diatoms in the family are adapted. Figure 1(b) shows the variation of ambient irradiance in the waveband 400–700 nm experienced by family 83002, and the irradiance to which it is adapted (an effect previously studied by Marra, 1978; Falkowski and Wirrich, 1981; Denman and Marra, 1986; Lewis *et al.*, 1984; Lande and Lewis, 1989). Diatom respiration reduces the energy pool at every time step, day and night. Figure 1(c) compares the rates of energy gain from photosynthesis and loss by respiration for every diatom in family 83002. So the energy level in the pool experiences a diurnal modulation, rising during the day and falling at night. During days of high ambient irradiance the level rises rapidly until it reaches the threshold for reproduction, when every diatom in the family divides, thereby doubling the population in the family. Figure 1(d) shows the

Figure 1. Audit trail of a diatom in family 83002 from 8 to 12 April. (a) Depth of the diatom. The water is turbulent in the shaded mixing layer bounded below by the turbocline. The mixed layer is defined as the daily maximum depth of the turbocline. (b) Ambient irradiance (400–700 nm) and photo-adaptation irradiance. The hours of sunlight are indicated by shading under the ambient irradiance curve. (c) Rate of energy gain by photosynthesis and energy loss by respiration. (d) Energy pool of the diatom. Cell division occurred at 17:00 on 8 April when the energy pool exceeded the threshold for reproduction.

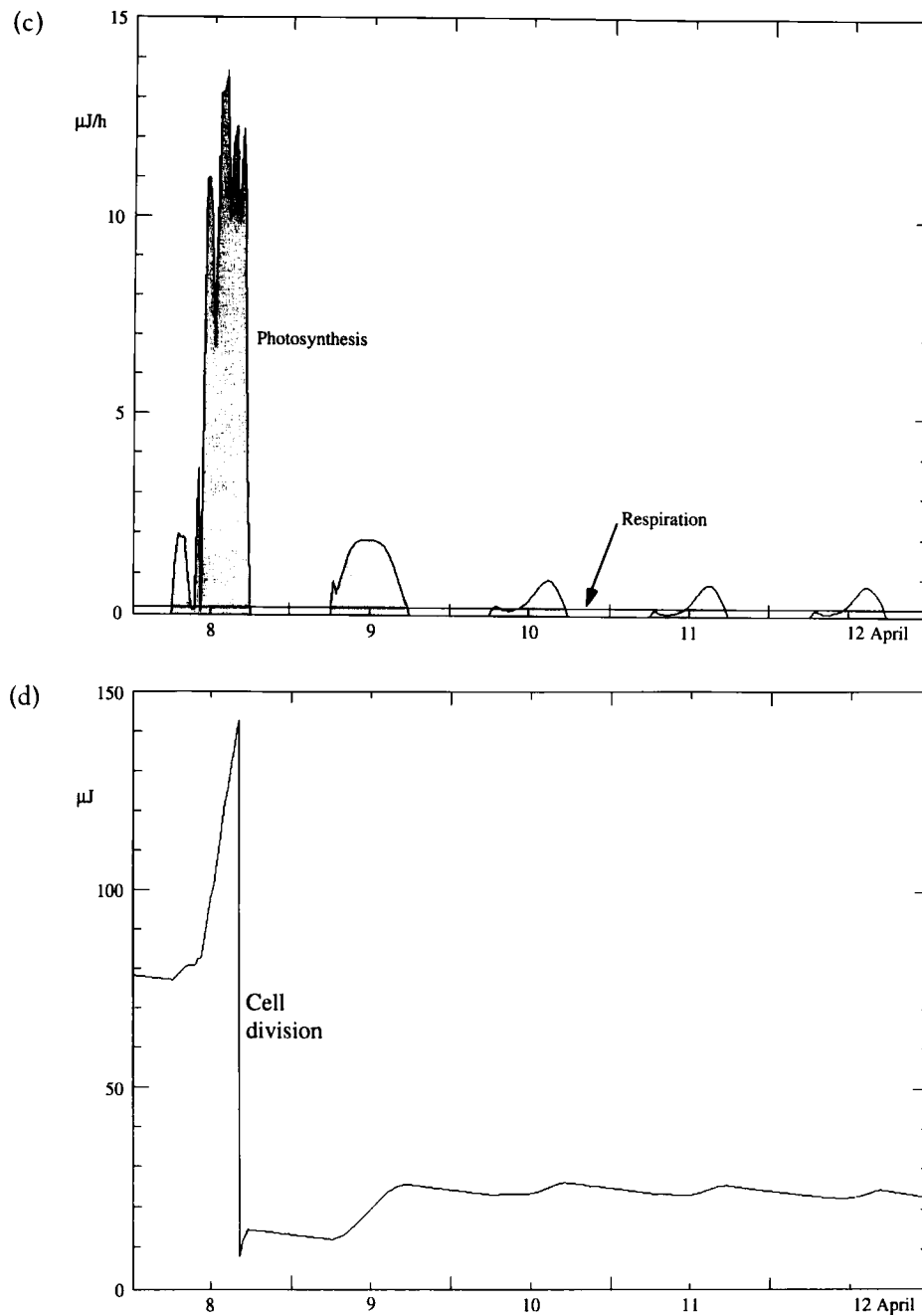


changing level of the energy pool in the family 83002, in which all diatoms reproduce at 17:00 on the 8 April. In our model, cell division occurs only during the hours of daylight (see discussion by Chilsolm *et al.*, 1980).

New cells are the same size as old cells; they contain 460 pg of carbon and 140 μ J of energy.

A reproduction event causes a sharp fall in the energy pool, bringing it close to zero. The criterion for the

Figure 1. (cont.)



family to die is that the energy pool becomes negative, so reproduction is a life-threatening event. Provided reproduction occurs in bright sunlight (as in Fig. 1d), the energy gain from photosynthesis exceeds the rate of loss by respiration sufficiently to raise the level of the energy pool high enough to cope with the decline during the next night. However if reproduction occurs in dim light (deep in the water column or just before

sunset), the energy pool may not be able to cope with respiration during the night, in which case the family will die. When that happens all diatoms in the family die simultaneously, regardless of their age. Death is a family catastrophe. It cannot be predicted more than a few hours ahead, because it depends on the rate of energy uptake which depends on turbulent mixing, a process treated as random in our model.

Clans and families of diatoms

In the earliest models based on the Lagrangian Ensemble method (Woods and Onken, 1982), the initial number of families was small and the population of diatoms in the mixed layer became rapidly depleted because families died out. That was an artefact of the model that had to be remedied before we could simulate the diatom population reliably through integrations extending over many years. Solving that problem was a prerequisite for studying the population in winter when energy gain by photosynthesis is low. The problem arises because it is not possible to integrate the biological equations separately for every diatom in the population, which exceeds 1 million m^{-2} even in winter off Greenland (Fig. 4). The Lagrangian Ensemble method groups the population into families and integrates the biological equations independently for each family. The problem of premature extinction was an artefact of that computational method and was addressed by modifying it to allow families to split, sharing their population of diatoms, whenever the population of families became too low. Note that this process of splitting families is merely a computational process to ensure that the Lagrangian Ensemble method handles the diatom population correctly. Splitting occurs automatically in the model whenever the population of families falls below 20 in any 1 m thick layer of the model. One can think of each layer containing 20 niches, all of which must be filled by at least one family. When there is vacant niche, half of the diatoms in the largest family in the layer are exported into a new family, which thereafter follows its own independent trajectory.

A register is kept of all splitting events, with the family labels of old and new. Analysis of this register permits a genealogical analysis of family histories, tracing each family back through a sequence of splitting events to the original family from which it grew. The set of original families established when the integration was started are called clans. Every family belongs to one of the initial set of 4000 clans. Some clans die out early in the integration; others survive through their descendent families to the end of the integration. The computational trick of splitting ensures that the population of diatoms does not become artificially depleted by family deaths.

Figure 2 shows the complete genealogical record for clan 16, which was created on 1 March when the model integration began, and ended on 5 May with the demise of the last surviving descendent family. Each family is represented by a set of bars, the top one starting with the import of diatoms by a splitting event and ending with the death of the family. The other bars in the family set

start with a reproduction event. The table on the right records the number of diatoms imported, created and exported. The fact that the numbers deviate slightly from powers of two reflects losses to grazing.

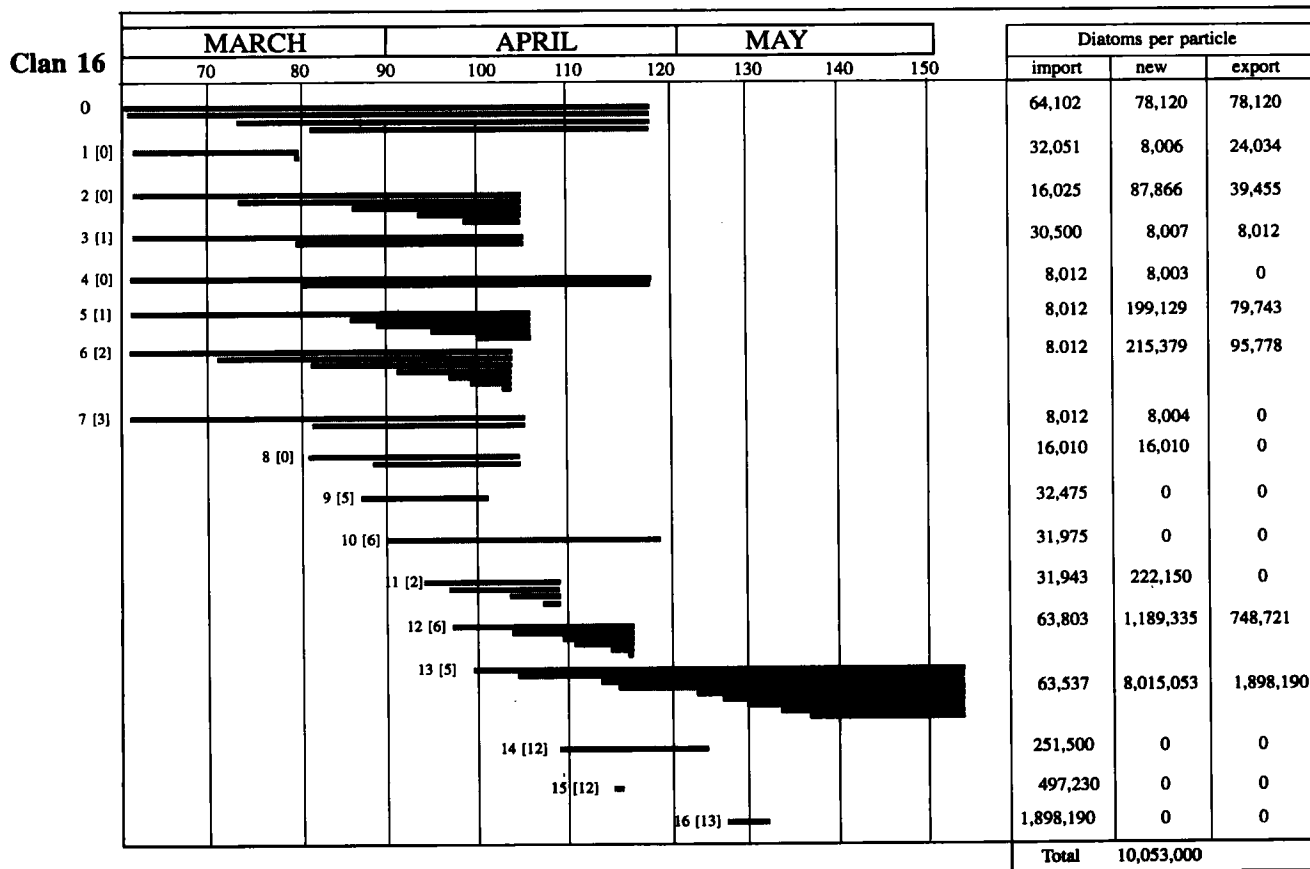
Let us examine some of the family histories. The clan leader, 16/0, started with 64 102 diatoms, enjoyed three reproduction events and ended with 78 120 new diatoms, having exported 78 120 to other families (16/1, 16/3, 16/4 and 16/8). Family 16/1 received 32 051 diatoms from 16/0 on 2 March, and enjoyed a reproduction event on 19 March which proved fatal the next night. Family 16/4 received 8012 diatoms from 16/0 on 2 March, doubled the number by reproduction on 20 March and survived until 27 April without being split, but having lost 7 diatoms to grazing. The most prolific family (16/13) inherited 63 537 diatoms from 16/5 on the 9 April, enjoyed eight reproduction events creating 10 million new diatoms, of which 1.9 million were exported to 16/16 on 7 May. The total production of the clan was dominated by two families (16/12, 16/13).

The most remarkable feature of this clan history is the diversity in family history. It is essential to maintain as large a number of families as possible in order to avoid introducing a bias into the statistical analysis of population dynamics. And it is important to bear in mind this diversity, revealed by Lagrangian analysis of the population, when interpreting Eulerian averages which combine the attributes of different sets of families. We have investigated the sensitivity of our results to the number of clans, and conclude that 4000 is sufficient, given the power of the splitting routine to maintain a sufficient concentration of families throughout the integration.

SEASONAL VARIATION OF TURBULENCE

The seasonal cycle in turbulent mixing lies at the heart of the problem of plankton demography (Tett and Edwards, 1984; Yamazaki and Osborn, 1988; Kiørboe, 1993). It is essential to simulate realistically the diurnal and seasonal variation of the depth of the mixing layer (Federov and Ginzburg, 1992; Lewis *et al.*, 1984; Taylor and Stephens, 1993). Our model incorporates the Woods and Barkmann (1986) treatment of turbulence in which buoyant convective adjustment and turbulent entrainment are computed separately in diagnosing the depth of the turbocline at each time step. This leads to realistic simulation of the diurnal variation of turbocline depth, which has a minimum at noon every day (diurnal change is controlled astronomically, because changes of weather are not included). The turbocline descends from noon until it reaches a daily maximum depth about an hour after sunrise, when the solar

Figure 2. History of families in clan 16, showing the timing of formation by splitting, cell division and death. Each family is represented by a horizontal line extending from formation by splitting to death by energy exhaustion. It is labelled with its own family number and in parentheses that of its parent family. The table shows the number of diatoms in each family when it was formed, the number of new diatoms created by cell division and the number exported to other particles by splitting.



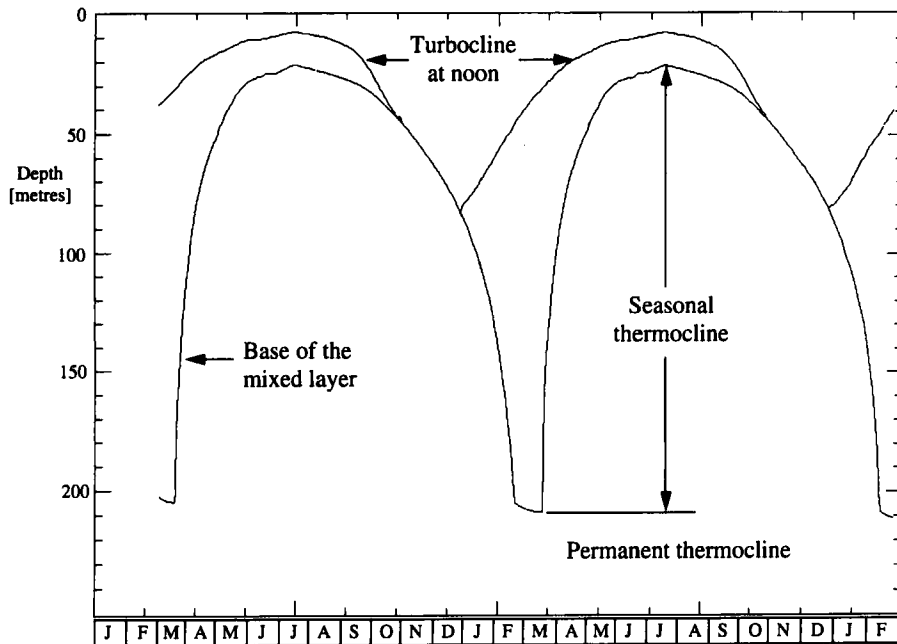
heating rate first exceeds the ocean heat loss to the atmosphere. In autumn, as the days get shorter, the diurnal rise of the mixing layer gets later and later until it stops completely between mid-November and the winter solstice (off the Azores; the precise period of no diurnal variation in turbocline depth depends on location). The daylength increases after the winter solstice. The increasing solar heat input soon becomes sufficient to quench convection, allowing the turbocline to rise above its daily maximum depth for a progressively longer period about noon each day (Woods, 1980).

The model assumes that the flow is laminar below the turbocline. That is consistent with flow visualization observations (Woods, 1968). At every time step, the model calculates the rate of power supply to the turbulence above the turbocline from potential energy released by buoyant convection and from the windstress (see Woods and Barkmann, 1986, for details). Power

input (P) is typically of order mW m^{-3} , as measured by Oakey and Elliott (1982). The turbulence is assumed to be continuous and uniform above the turbocline. At each time step the height of the energy-containing eddies is assumed to equal the turbocline depth (h). The overturning time (T) for those eddies can be estimated from the power input and height as follows: $T = (h^2/P)^{1/3}$, which is typically 20 min. That is shorter than the half-hour time step of the model, so there is no need in this model to take account of coherent eddy structure, as was done by Woods and Onken (1982), who used 10 min time steps.

At each time step of the model integration, every family acts as a particle which changes its depth in response to a combination of turbulence and its own behaviour (sinking or swimming). Turbulent displacement only applies above the turbocline. In that mixing layer a family is displaced randomly to a new depth

Figure 3. Seasonal variation of the daily maximum and minimum depths of the turbocline.



between the sea surface and the turbocline. Then the model adjusts the new depth according to the family's movement relative to the water by sinking or swimming. Finally the model diagnoses the new depth of the turbocline. If the turbocline has become shallower, those families with depths between the old and the new turbocline depths now lie in laminar flow below the mixing layer; they will not experience turbulent displacement at the next time step.

Dissolved chemicals are assumed to be always well mixed above the turbocline and subject to zero vertical diffusion below it. That is a synoptic statement valid within one time step of the integration: longer-term vertical diffusion of dissolved chemical depends on entrainment into the mixing layer (when the turbocline descends) and subduction into the thermocline (when it ascends). This process is realistically simulated by the model.

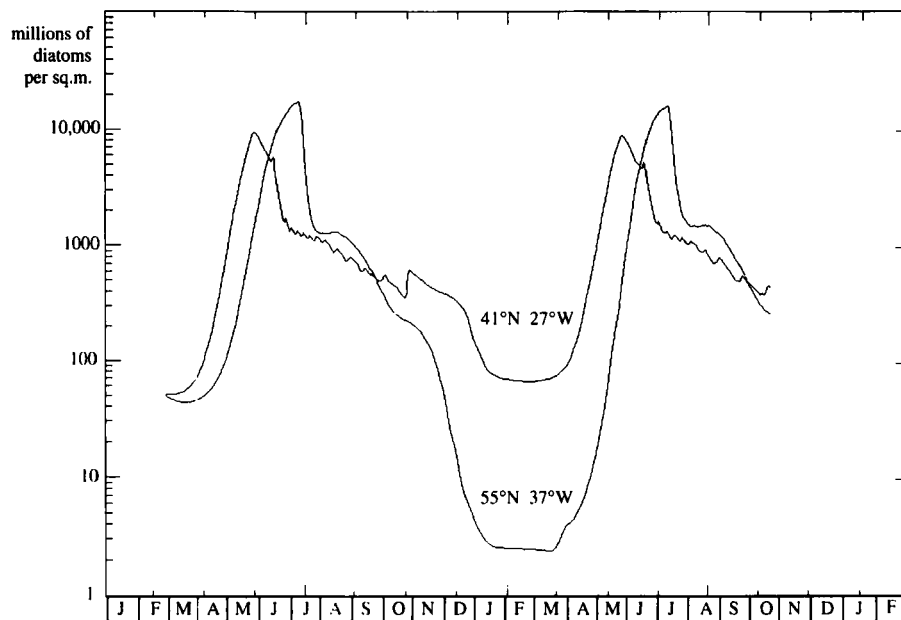
Figure 3 shows the variation of daily minimum and maximum depths of the turbocline. The turbocline is the interface across which turbulence decreases from order $mW m^{-3}$ to zero; it is not a material surface. The mixing layer comprises all the water above the turbocline. The mixed layer comprises all the water between the last diurnal maximum depth of the turbocline and the surface; that water has been mixed in the last 24 h. The diurnal thermocline contains all the mixed-layer water lying below the turbocline. The seasonal thermocline contains the water between the daily and annual

maximum depths of the turbocline. The permanent thermocline contains the water below the annual maximum depth of the turbocline; that water is never mixed vertically at the fixed location of the (geographically Eulerian) integration. The flow in all three thermoclines is assumed to be laminar. Flow visualization observations (Woods, 1968) show that in fact there are sporadic, small-scale turbulence events in the thermoclines, with concentration largest during the morning in the diurnal thermocline and smallest in the permanent thermocline. The energy-containing eddies of those rare events are smaller than 1 m, so they do not significantly displace particles on the time scales of interest in this paper. It is also reasonable to neglect vertical diffusion of dissolved chemicals in the thermoclines.

SEASONAL VARIATION OF THE DIATOM POPULATION

Figure 4 shows the variation of diatom population off the Azores and off Greenland. The Azores population falls from 400 million diatoms m^{-2} in December to 70 million at the end of February, and rises to ten billion at the peak of the bloom in April. The Greenland population reaches a higher peak in the spring bloom (eighteen billion m^{-2}) and descends below 3 million at the end of February. The annual maximum population at 55°N lags that at 41°N by 1 month, but the minimum

Figure 4. Seasonal variation of the number of diatoms in a water column 1 m² in cross section at two sites: (i) 41°N, 27°W and (ii) 55°N, 37°W.



occurs on the same day at both sites, suggesting that it is controlled astronomically, i.e. at the winter solstice when the daylight starts to increase. The numbers of diatoms in the simulated annual cycle are similar to those observed at OWS "I" by Corlett (1953).

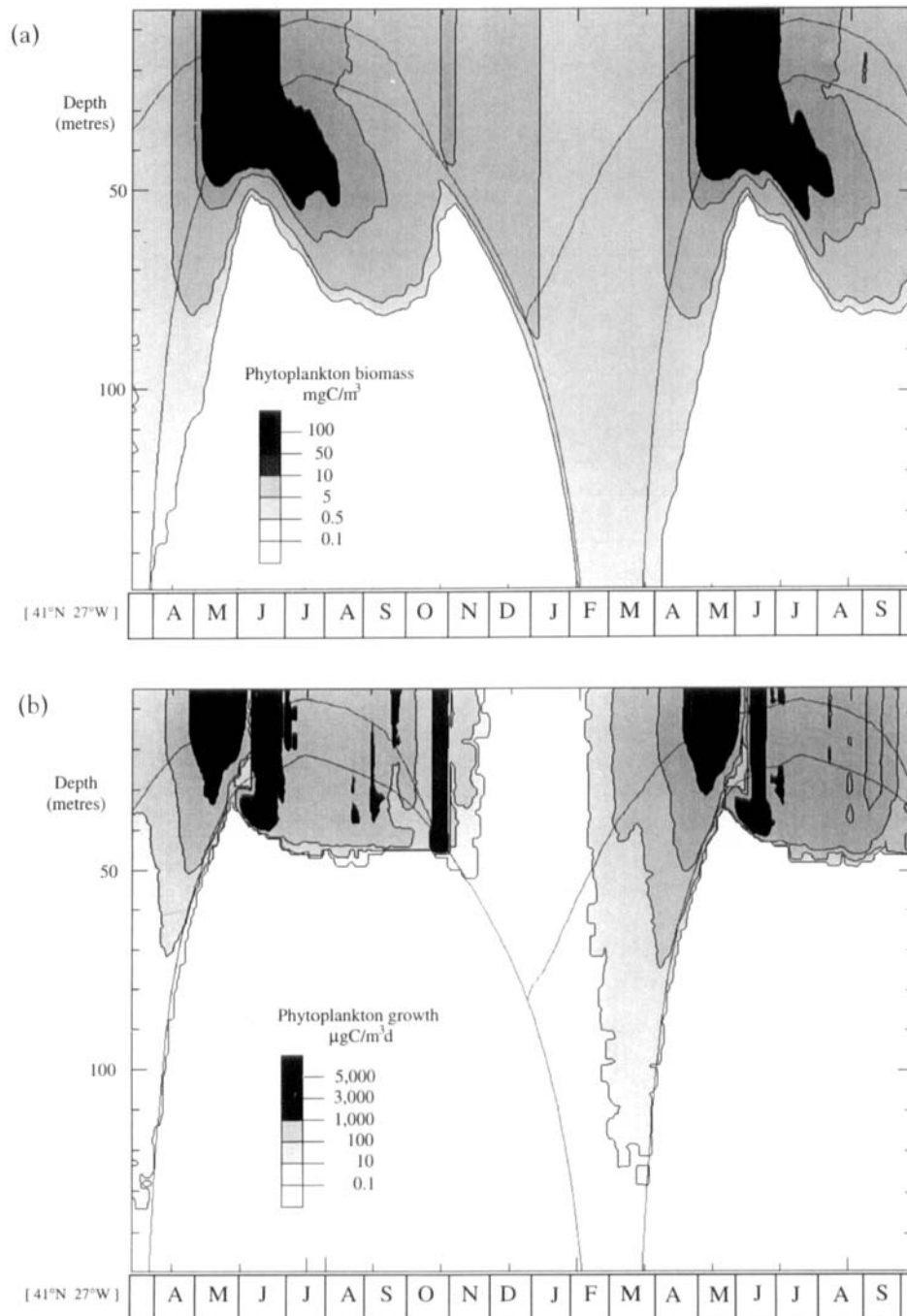
Figure 5(a) shows the vertical distribution of the phytoplankton biomass off the Azores. Taking a threshold of 0.5 mgC m^{-3} for the onset of the spring bloom it begins on 8 April when the mixed layer is 80 m deep. According to Sverdrup's criterion, that suggests the critical depth should be 80 m. However, Fig. 5(b) shows that phytoplankton growth began about 6 weeks earlier when the mixed layer was 200 m deep. The trigger for growth was ascent of the diurnal thermocline to 50 m, trapping diatoms in the mixing layer above it in the way envisaged by Sverdrup. That explanation is confirmed by the vertical distribution of cell division rate (Fig. 5c), which has a maximum above the noon depth of the thermocline during March and April.

Population change depends on the balance between birth rate and life expectancy. We have seen that the diatom birth rate begins to increase in late February. Their life expectancy can be estimated from the daily mortality (Fig. 5d). Remembering that the criterion for family death is that the energy pool becomes depleted, it is not surprising that the shortest life expectancy, less than 3 d, occurs at the base of the population, when it lies in the seasonal thermocline in laminar flow. Death

occurs mainly to diatoms that have been subducted into the seasonal thermocline as the mixed layer rises, or that have fallen into it in summer. The sharply defined band of high mortality is shaped by self shading, which cuts off the light supply to photosynthesis when the population is high enough from April to October inclusive. From November to March the mixed layer deepens faster than the fall speed of the diatoms so the population is re-entrained into the turbulent regime each night; their life expectancy is vertically homogeneous.

The actual value of life expectancy in winter is sensitive to the algorithm used in the model for respiration. We follow normal practice in reducing respiration rate with temperature. Experience has shown that is not sufficient to ensure survival of the diatom population in winter, so we also reduce respiration rate with population density according to a Michaelis-Menton relation (see Appendix). That is no more than a mathematical convenience: there is no scientific reason for believing that diatom respiration depends on the proximity of its neighbours. So we have also investigated an alternative algorithm in which respiration decreases with irradiance, which is of course low in winter when the days are short and particles are mixed into deep water (Harris, 1980). Although there are some slight differences between these two approaches, they both produce a maximum life expectancy in February that is longer than the 10 weeks for the winter

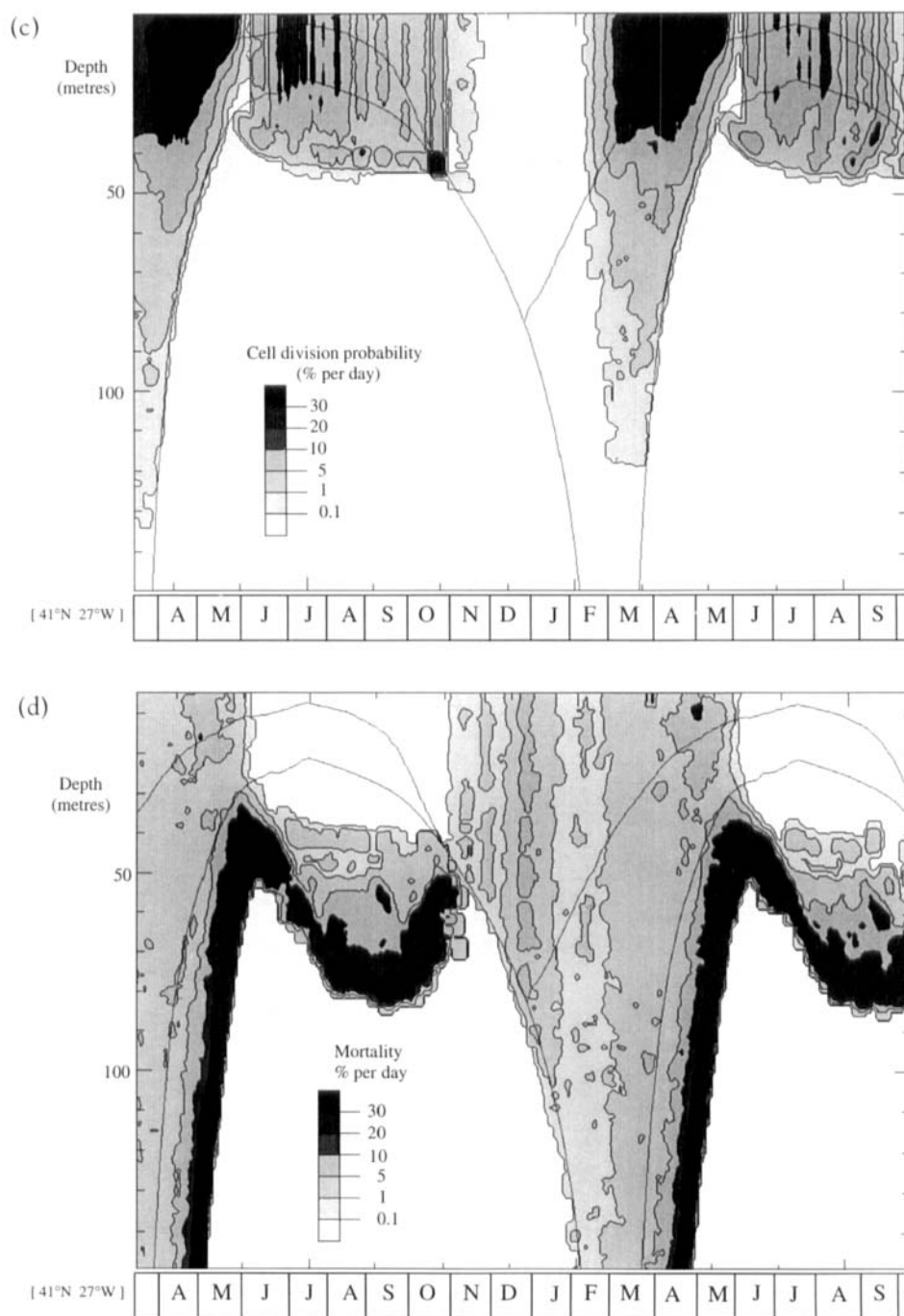
Figure 5. Vertical distribution of seasonally changing diatom population. (a) Phytoplankton biomass. (b) Rate of increase of biomass by cell division. (c) Cell division rate. (d) Fraction of the population dying each day owing to natural mortality. (e) Net daily primary production, defined as the rate of cell division minus the rate of natural mortality in each 1 m thick layer of the model each day.



solstice when the birth rate is negligible. Further research is needed to develop an improved algorithm for winter respiration, involving more than the well-established temperature dependence; see Geider (1992) for a recent review of the subject.

Figure 5(e) shows the net production, defined as growth rate (Fig. 5b) minus natural mortality (Fig. 5d). Net production and growth rate are similar where natural mortality is negligible, notably in the mixed layer during the summer oligotrophic phase. But they

Figure 5. (cont.)



differ in May when self shading causes high mortality in the lower reaches of the mixed layer. As in Fig. 5(a–d), the structure in the second year closely matches that in the first year, showing that the model simulates a diatom population in balance with its seasonally changing environment.

Finally we confirmed that grazing is not a significant

factor controlling the winter population of diatoms. Figure 6 shows that the total loss to grazing is less than $0.1\% \text{ d}^{-1}$ throughout the winter. Of course, adequate grazing is important for survival of the population of herbivores, and we have confirmed that even though the rate is low in winter, it is sufficient to maintain a stationary population of zooplankton for 20 y, albeit

Figure 5. (cont.)

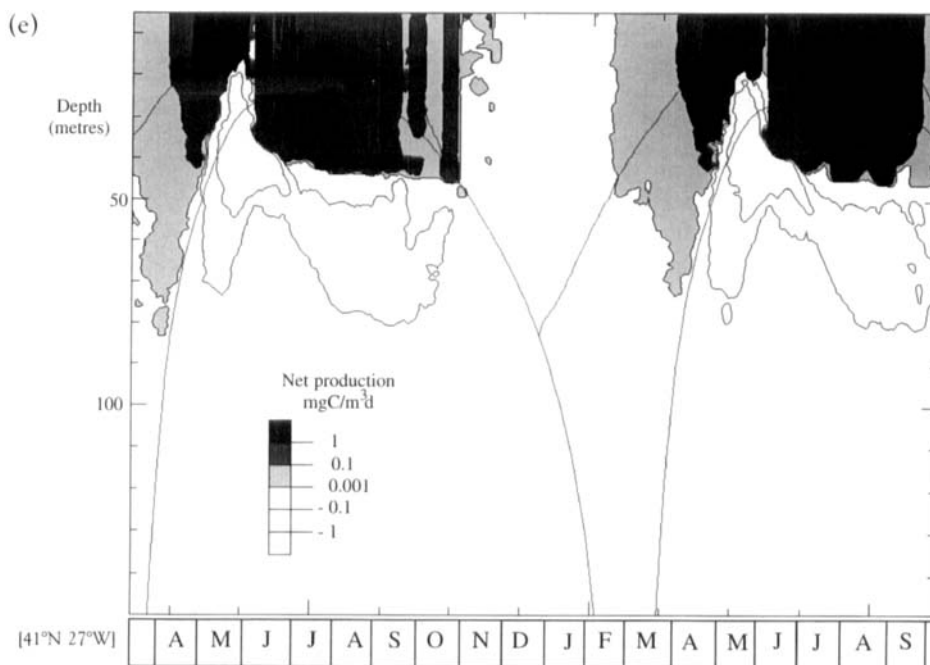
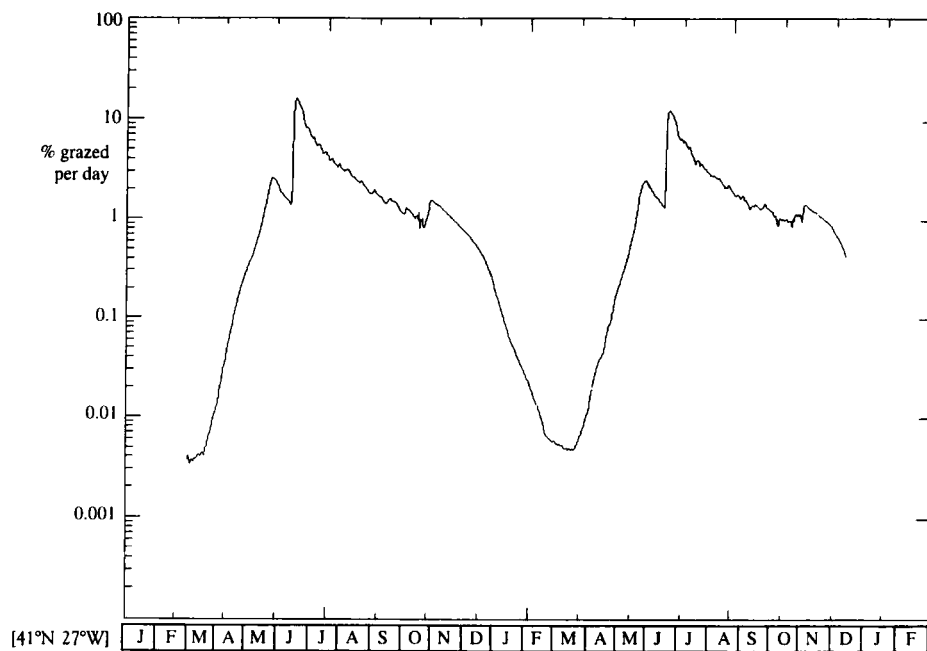


Figure 6. The fraction of the diatom population lost each day to grazing.



with significant interannual variability. We have not carried out long integrations at the other site (55°N, 37°W) where the diatom population is much lower, which may present problems for zooplankton survival (Fasham, 1992).

Chilsolm *et al.* (1980) have considered the diurnal variation of cell division rate. In our model cell division occurs during the day. In late winter the simulated concentration of living diatoms is about 30% higher in the afternoon, which may offer a feeding opportunity to

herbivores that modulate their diel migration accordingly. In our model they do not rise until sunset, by which time the turbocline is descending, diluting the concentration of new diatoms. We hope to be able to report our investigation of the winter population of zooplankton soon.

We do not believe that the neglect of other guilds of phytoplankton significantly affects the ability of our model to simulate the changing population of diatoms in winter. Other guilds are likely to involve smaller organisms that have a negligible influence on the vertical distribution of light, and the competition for nutrients by other guilds does not become a limiting factor for diatoms in winter. The termination of the spring bloom by nitrate depletion is simulated by our model (Wolf and Woods, 1988) but it occurs after the light-limited processes that are the subject of this paper.

CRITICAL DEPTH AND COMPENSATION DEPTH

Sverdrup (1953) defined the critical depth (Z_{critical}) for a phytoplankton population in the mixed layer as the depth of the mixed layer above which the population would increase, because it gains more energy from photosynthesis than it loses to respiration. For a recent discussion of the theory see Platt *et al.* (1991). Some authors (notably Tett, 1990) have argued that the compensation depth ($Z_{\text{compensation}}$) may be a more useful predictor for the bloom. Here we report the results of calculating both critical depth and compensation depth from the data generated by our model, and discuss their value for predicting winter changes in diatom population simulated by the model.

Critical depth

Some authors have calculated the seasonal variation of Z_{critical} from the irradiance profile and assumptions about the energy balance of a hypothetical homogeneous population of identically adapted phytoplankters (see, for example, Fig. 2.5(c) in Valiela, 1991). The result is a critical depth that descends from the winter solstice to the summer solstice. That simple calculation is based on a number of assumptions that are no longer necessary when one has available detailed information about the vertical distribution of all relevant variables (Table 1). For example, it is no longer necessary to assume a hypothetical homogeneous population: the vertical integral used to compute Z_{critical} should be based on the known vertical distribution of phytoplankton, thereby avoiding the inconsistency of diagnosing a critical depth at which there are no plankton.

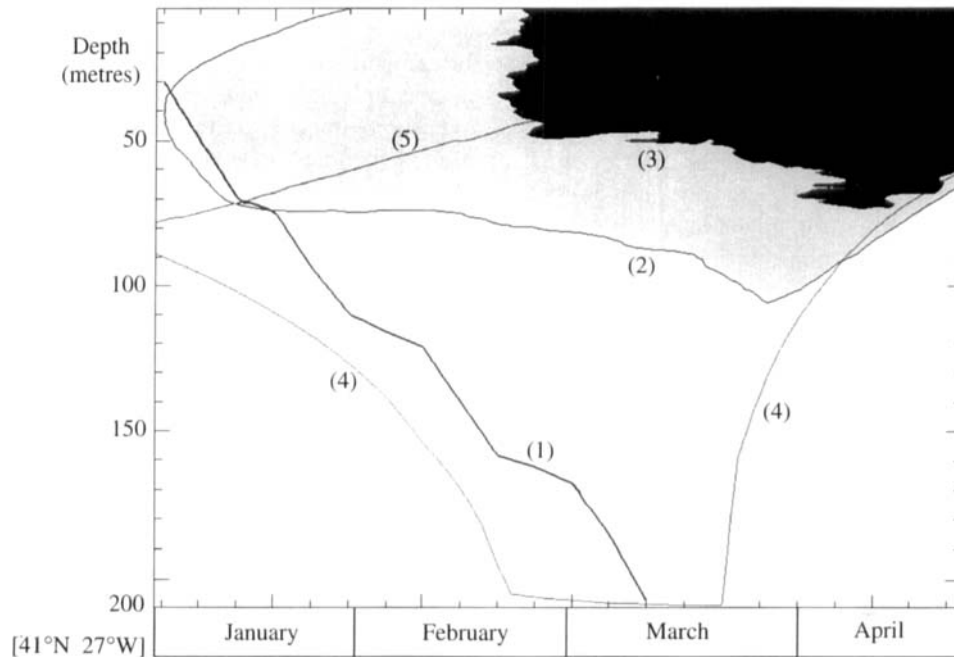
Furthermore, our model calculates the vertical profile of photosynthetically active radiation (PAR) from a 27-waveband spectrum with turbidity controlled not only by the seawater but also by the plankton concentration; that means that we do not have to invoke the simplifying assumption that PAR varies exponentially with depth. The LE method allows us to compute the actual energy uptake of the population of diatoms, allowing for their vertical mixing and photo-adaptation – effects neglected in classical calculations of critical depth. And finally our model includes the effect of diurnal variation of the depth of the mixing layer, which is normally neglected in computing critical depth. The question to be addressed in this section is whether the critical depth computed from the information available to us from our model provides a useful predictor of population changes as it does in the classical theory based on simplifying assumptions.

The initial scientific problem is how properly to calculate the critical depth for a vertically inhomogeneous population of phytoplankton. In classical theory the population is homogeneous, and the critical depth is defined in terms of a population in the mixed layer at the moment when they are the same. Seasonal variation of the critical depth is a theoretical concept that can only be extracted from our model by creating artificial conditions corresponding to those required by the definition. We have therefore run the model 16 times with different fixed mixed layer depths (H) in the range 30–200 m, in order to diagnose in each case the date on which the critical depth (calculated for the population of diatoms in the mixed layer) equals the mixed layer depth. The results have been combined to give the variation of critical depth in winter shown in Fig. 7, together with curves for compensation depth (to be discussed later) and daily minimum and maximum depths of the turbocline from the standard model integration (i.e. with dynamic mixed layer depth) replotted from Figs 5(e) and 8(c). The critical depth descends during winter, but much more sharply than in Valiela's (1991) calculation. It does not cross the rising mixed layer depth at 80 m on the 9 April, as would be expected from Sverdrup's criterion. We conclude that not only is the critical depth difficult to diagnose in our model data, but that even when extracted from a special set of integrations designed to be consistent with Sverdrup's definition, the critical depth curve does not intersect the rising mixed layer depth, so it cannot be used as a criterion for predicting population dynamics.

Compensation depth (energy pool)

That leads us to consider the merits of compensation depth as a predictor of population change. The compen-

Figure 7. Winter variation of (1) critical depth, (2) compensation depth for energy pool, (3) compensation depth for cell division, (4) mixed layer depth, and (5) noon depth of the diurnal thermocline.



sation depth is defined as the depth at which plankters are gaining as much energy from photosynthesis as they are losing from respiration. We have to be careful about how we calculate compensation depth, because there is a wide variation in the rate of energy gain by diatoms at the same depth, even though they have the same ambient irradiance. The variety is caused by differences in the photo-adaptation of plankton that have arrived at the chosen depth along different trajectories and experienced different histories of ambient irradiance during the last 2 d†. We calculated the vertical distribution of the daily energy budget of the diatom population by taking Eulerian averages of all diatoms in each 1 m thick layer for all 48 time steps in one day. Such Eulerian averaging involves combining data from different samples of the diatom population as they pass through the chosen layer, but it provides the closest approximation to the classical definition of compensation depth.

Figure 8(a) shows the seasonal variation of the vertical distribution of daily mean energy gain per diatom. The minimum gain is centred on the winter solstice, when it falls to less than $5 \mu\text{J d}^{-1}$. Note the curvature of the contour for $5 \mu\text{J d}^{-1}$, which is due to photo-adaptation, about which we shall have more to say later.

† The e-folding time for photo-adaptation in our model is 8 h.

Figure 8(b) shows that corresponding distribution for energy loss by respiration, which has a minimum in late February when the population density is lowest, for reasons discussed earlier.

Combining these two distributions, we get the seasonal variation of the vertical distribution of mean net daily energy balance. By definition the compensation depth is the contour for zero net energy balance. Figure 8(c) shows the compensation depth, which lies at the base of the shaded area in which on average diatoms are gaining energy‡. Note that the compensation depth surfaces for the months of November, December and January. During that period diatoms consistently lose energy and many die. Note that no diatom can cover the demands of 3 months respiration (approximately $240 \mu\text{J}$) from its stored energy reserve, which cannot exceed $140 \mu\text{J}$ (Fig. 1d); if it is to survive from November to February it must gain at least $100 \mu\text{J}$ from photosynthesis. Seventy million diatoms m^{-2} do achieve that target (Fig. 4) and they provide the initial population for the next growing season. Note the curvature on the nearly vertical compensation depth curve in November and January: that is due to photo-adaptation.

‡ The same curve is drawn in Fig. 7.

The most striking feature of the compensation depth curve is the rise from a little deeper than 100 m at the vernal equinox to 40 m 1 month later. That rise tracks the rise of the mixed layer during that month. The two curves appear to be locked together, i.e.:

$$Z_{\text{compensation}} = H \pm 5 \text{ m, for } 100 < H < 40 \text{ m (1)}$$

Remember that we earlier identified the start of the spring bloom (by the 0.5 mgC m^{-3} criterion, Fig. 5a) as occurring on 8 April when the mixed layer was 80 m deep. The winter change of compensation depth cannot be used to predict that event.

The reason for this unexpected result lies in the difference between the energy uptake of the diatoms in the mixed layer and those in the seasonal thermocline at the same depth and therefore exposed to the same ambient irradiance. The difference in energy uptake is due to the difference in photo-adaptation of particles trapped in the seasonal thermocline compared with those in the mixing layer. Figure 9 shows the sharp drop in the Eulerian average energy uptake at 80–81 m as the base of the mixed layer rises through that layer on 8 April. We got the same result using a different algorithm for photo-adaptation (symmetric rather than asymmetric). The difference is caused by photo-adaptation, but does not depend on the algorithm. Rather, it depends on the ambient irradiance histories of the diatoms during the preceding 2 d which contributed to their state of photo-adaptation (Fig. 1). The ambient irradiance history of a diatom depends on its trajectory during that period. The trajectory of a diatom in the seasonal thermocline is not affected by turbulence: it descends smoothly at 1 m d^{-1} . Its adaptation irradiance undulates diurnally with a 4 h phase lag relative to the diurnal variation of ambient irradiance. At a depth of 80 m (Fig. 1d) the level of the diatom's energy pool slowly decreases each day. It therefore, by definition, lies below the compensation depth.

By contrast, a diatom that lies in the mixed layer has a trajectory history that may extend randomly through the full depth range of the mixed layer. In April the mixed layer is rising at 2 m d^{-1} , so diatoms at the base of the mixed layer on a particular date could not have been more than 4 m deeper during the previous 2 d when their ambient irradiance history was contributing to their adaptation irradiance. So a diatom in the depth range 80–81 m on 8 April lies just inside the mixed layer, but has a photo-adaptation which records its history of ambient irradiance at much shallower depths during the previous 2 d. That makes it much better able to exploit the energy supply that day, so the level of its energy pool rises. A diatom in the same depth range on 9 April has been subducted into the seasonal thermo-

cline, but it spent the last 2 d in the mixed layer so it still has a relatively high photo-adaptation irradiance. That matches the ambient irradiance quite well, so the level of its energy pool rises in that 24 h period: it lies above the compensation depth. But by 11 April it has lost its memory of high ambient irradiance in the mixed layer, and can no longer cover the energy loss through respiration; it then lies below the compensation depth.

This explanation of the tight relationship between compensation and mixed layer depths applies not only at 80 m but at all depths from 100 to 40 m. We therefore conclude that it is inevitable that the compensation depth will track the mixed layer as it rises in spring.

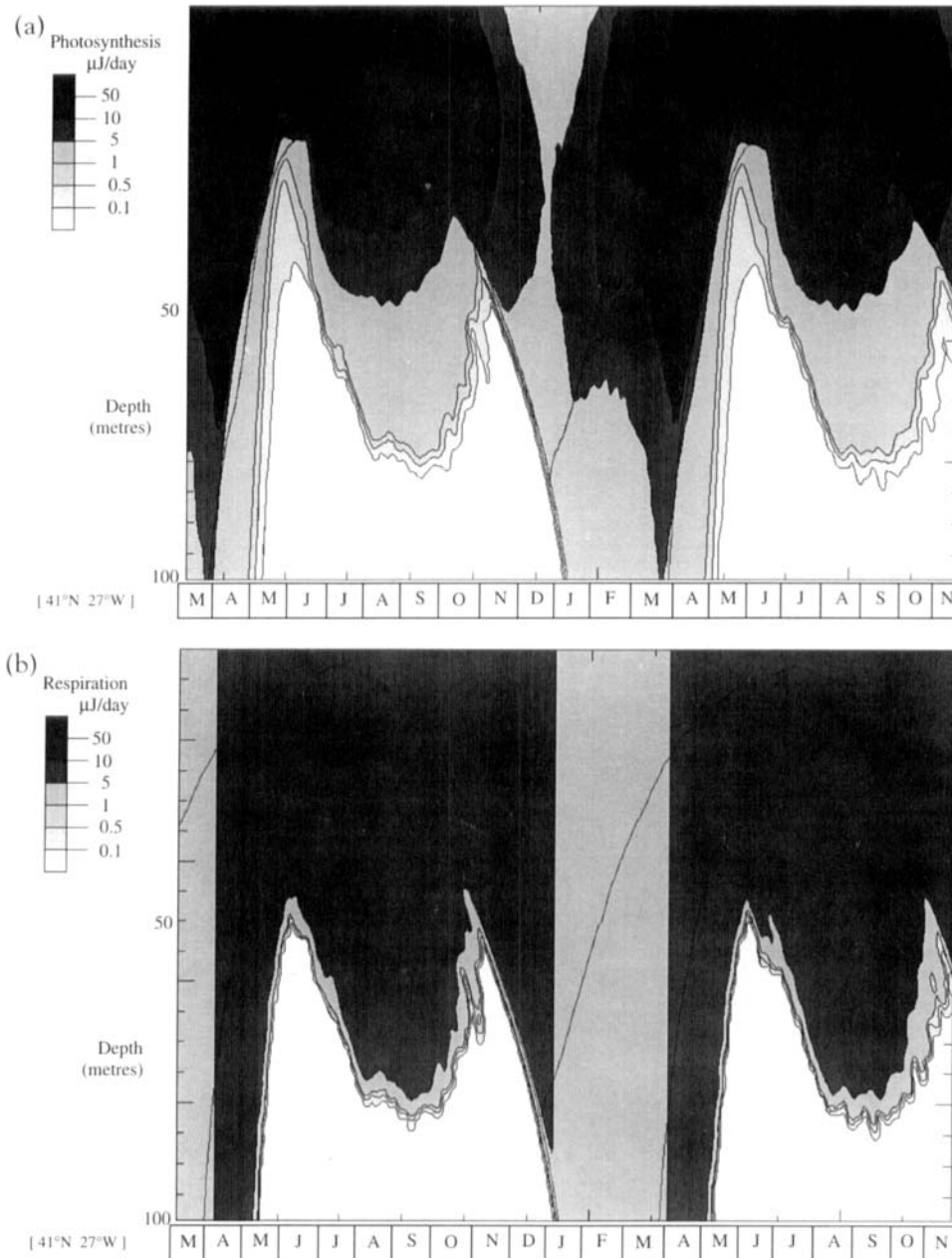
As the diatom population increases, it begins to control the turbidity of the water, and self shading causes the compensation depth to rise evenly faster than the mixed layer until late May, when compensation = 23 m and $H = 30 \text{ m}$.

Compensation depth (cell division)

Finally we note that the seasonal variation of compensation depth shown in Fig. 8(c) is based on the daily mean change of the energy pool in the diatoms encountered at each 1 m thick layer. That is particularly relevant to the problem of vertical distribution of mortality. As we noted earlier, most diatoms die in the seasonal thermocline. If the aim is to relate energy balance to changes in population, it is important to take account not only of death rate, but also birth rate. The changing level of the energy pool is not an accurate predictor for birth rate, which depends on the frequency with which it exceeds a threshold value ($140 \mu\text{J}$). The vertical distribution of birth (cell division) rate was shown in Fig. 5(c), and Fig. 5(e) shows the net growth rate, defined as the rate of generation of new biomass by cell division minus the loss of biomass by natural mortality. The shaded regions in Fig. 5(e) show where the population is growing. That leads to an alternative definition of compensation depth, based not on the rate of change of diatom energy pool, but on those diatoms in which the energy pool passed the threshold for cell division. That tighter definition of compensation depth is better matched to the needs of a predictor for population change. It cannot be related to Sverdrup's criterion *sensu stricto* because it never crosses the rising mixed layer depth, but it does cross the rising noon depth of the turbocline on 20 February, when the diatom population starts to recover from the stress of winter.

Figure 7 compares the two versions of compensation depth (based on the energy pool and cell division respectively) with the critical depth and the depths of the mixed layer and diurnal thermocline.

Figure 8. Vertical distribution of seasonally changing energy balance of diatoms. (a) Mean daily energy gain per diatom by photosynthesis. (b) Mean daily energy loss per diatom by respiration. (c) Compensation depth based on daily mean energy balance.



CONCLUSION

We have used a mathematical model of the upper ocean ecosystem based on the Lagrangian Ensemble method to simulate the changes that occur in the population of diatoms during two years. The method permits detailed investigation of those changes from either a fixed (Eulerian) frame of reference or one that follows the trajectory of an individual diatom. That has allowed us

to clarify the energy balance responsible for changes in the diatom population and to consider separately the two factors that control demographic change: birth rate and life expectancy. We conclude that the birth rate begins to rise in late February (off the Azores) when the diurnal thermocline has risen to a depth of 50 m. The life expectancy of diatoms in the mixed layer does not vary much seasonally: most diatoms die after they have been subducted into or fallen into the seasonal thermo-

Figure 8. (cont.)

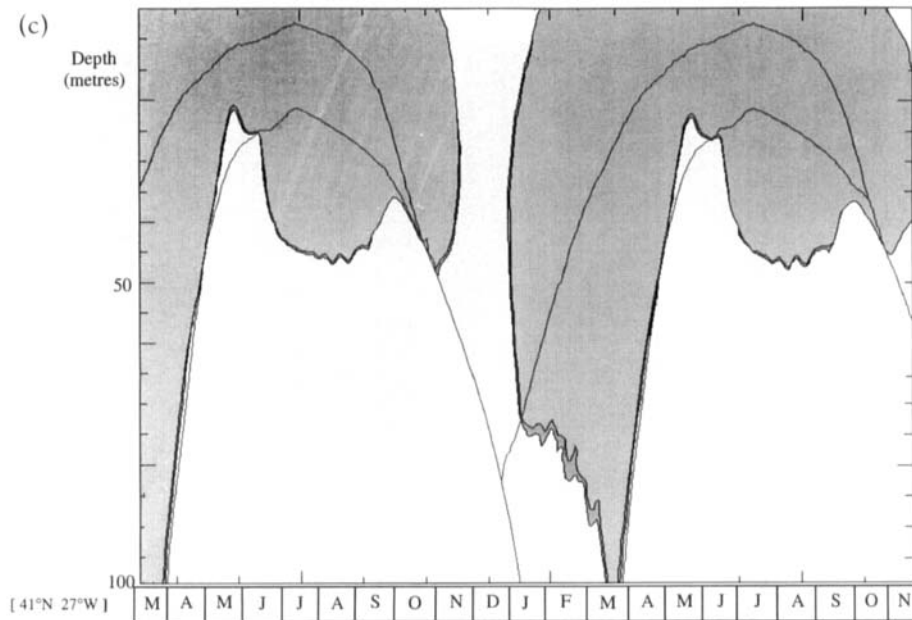
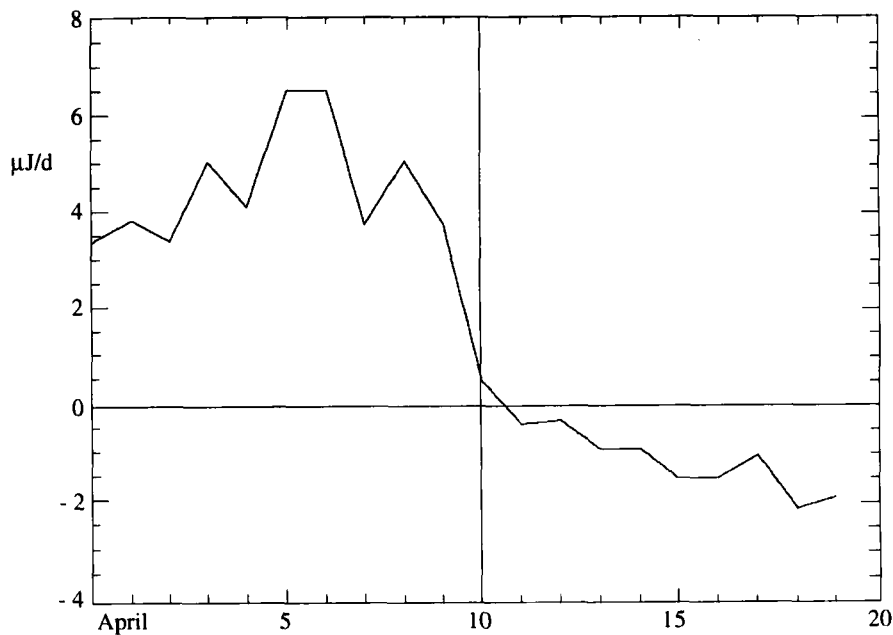


Figure 9. Mean daily net energy gain per diatom in the layer 80–81 m deep during the month of April at 41°N, 27°W.



cline. The Sverdrup criterion for the onset of the spring bloom does not provide a useful predictor for the population simulated by our model because the critical depth descends in winter without crossing the rising mixed layer depth. Nor is the compensation depth based on the diatom energy pool a useful predictor, because it tracks the mixed layer depth within 1 m as it rises from 100 to 40 m during 1 month after the vernal

equinox. Lagrangian analysis reveals that this is due to the higher mean adaptation irradiance of diatoms in the mixed layer than those at the same depth in the seasonal thermocline. The best predictor is provided by the intersection of the noon turbocline depth with the compensation depth calculated from the vertical distribution of net daily production.

ACKNOWLEDGEMENTS

We wish to thank David Cushing for his enthusiastic encouragement during the past 12 years as the Lagrangian Ensemble method was developed from its primitive early version described by Woods and Onken, and subsequently refined by Dr. U. Wolf and diploma students at the University of Kiel. Our LE'93 model used for the investigation reported in this paper was built on those foundations.

REFERENCES

- Bacastrow, R., and Bjorkstrom, A. (1981) Comparisons of ocean models of the carbon cycle. In: *Carbon Cycle Modelling*. B. Bolin (ed.). New York: Wiley, pp. 28–79.
- Chilsolm, S.W., Morel, F.M., and Slocum, W.S. (1980) The phasing and distribution of cell division cycles in marine diatoms. In: *Primary Productivity of the Sea*. P. G. Falkowski (ed.). New York: Plenum Press, pp. 281–300.
- Colebrook, J.M. (1979) Continuous plankton records: seasonal cycles of phytoplankton and copepods in the North Atlantic Ocean and North Sea. *Mar. Biol.* 51:23–32.
- Colebrook, J.M. (1985) Continuous plankton records: overwintering and annual fluctuations in the abundance of zooplankton. *Mar. Biol.* 84:261–265.
- Colebrook, J.M. (1986) Environmental influences on long-term variability in marine plankton. *Hydrobiologia* 142:309–325.
- Corlett, J. (1953) *J. Cons. Perm. Int. Mer.* 19:178–190.
- Cushing, D.H. (1975) *Marine Ecology and Fisheries*. London: Cambridge Univ. Press, 278 pp.
- Denman, K.L., and Marra, J. (1986) Modelling the time dependent adaptation of phytoplankton to fluctuating light. In: *Marine Interfaces: Ecohydrodynamics*. J.C.J. Nihoul (ed.). Amsterdam: Elsevier, pp. 341–359.
- Dickey, T., Marra, J., Granata, T., Langdon, C., Hamilton, M., Wigget, J., Siegel, D., and Bratkovich, A. (1991) Concurrent high resolution bio-optical and physical time series observations in the Sargasso Sea during the spring of 1987. *J. Geophys. Res.* 96(c5):8643–8663.
- Falkowski, P.G., and Wirrick, C.D. (1981) A simulation model of the effects of vertical mixing on primary productivity. *Mar. Biol.* 65:69–75.
- Fasham, M.J.R. (1993) Modelling the oceanic biota. In: *The Global Carbon Cycle*. M. Heimann (ed.). Berlin: Springer-Verlag.
- Federov, K.N., and Ginzburg, A.I. (1992) *The Near-surface Layer of the Ocean* (English edn.). Zeist: VSP, 259 pp.
- Geider R.J. (1992) Respiration: taxation without respiration? In: *Primary Production and Biogeochemical Cycles in the Sea*. P.G. Falkowski and A.D. Woodhead (eds). New York: Plenum Press, pp. 333–360.
- Harris, J.E. (1980) Respiration and photo-respiration in marine algae. In: *Primary Productivity in the Sea*. P.G. Falkowski (ed.). New York: Plenum Press, pp. 411–432.
- Isemer, H.J., and Hasse, L. (1986) *The Bunker Climate Atlas of the North Atlantic Ocean*. Berlin: Springer-Verlag.
- Kjørboe, T. (1993) Turbulence, phytoplankton cell size, and the structure of pelagic food webs. *Adv. Mar. Biol.* (in press).
- Lande, R., and Lewis, M.R. (1989) Models of photoadaptation and photosynthesis by algal cells in a turbulent mixed layer. *Deep-Sea Res.* 8:1161–1175.
- Lewis, M.R., Cullen, J.J., and Platt, T.R. (1984) Relationship between vertical mixing and photoadaptation: similarity criteria. *Mar. Ecol. Progr. Ser.* 15:141–149.
- Margelef, R. (1978) Life-forms of phytoplankton as survival alternatives in an unstable environment. *Oceanologica Acta*, 1:493–509.
- Marra, J. (1978) Effect of short term variation in light intensity on photosynthesis of a marine phytoplankton: a laboratory simulation study. *Mar. Biol.* 46:191–202.
- Marra, J., and Ho, C. (1993) Initiation of the spring bloom in the northeast Atlantic (47°N, 20°W): a numerical simulation. *Deep-Sea Res. II* 40:55–73.
- Oakey, N.S., and Elliot, J.A. (1982) Dissipation within the surface layer. *J. Phys. Oceanogr.* 12:171–185.
- Peng, T.-H., Takohashi, T., Broecker, W. S., and Olafsson, J. (1987) Seasonal variability of carbon dioxide, nutrients and oxygen in the northern North Atlantic surface waters: observations and a model. *Tellus* 39:439–458.
- Platt, T., Bird, D.F., and Sathyendranath, S. (1991) Critical depth and marine primary production. *Proc. R. Soc.* 264B:205–217.
- Raymont, J.E.G. (1980) *Plankton and Productivity in the Oceans: I. Phytoplankton*, 2nd edn. Oxford: Pergamon Press, 489 pp.
- Riley, G.A. (1942) The relationship of vertical turbulence and spring diatom flowerings. *J. Mar. Res.* 5:67–87.
- Strass, V.H. (1992) Chlorophyll patchiness caused by mesoscale upwellings at fronts. *Deep-Sea Res.* 39(1):75–96.
- Sverdrup, H. (1953) On conditions for the vernal blooming of phytoplankton. *J. Cons. Int. Explor. Mer* 18:287–295.
- Taylor, A.H., and Stephens, J.A. (1993) Diurnal variations of convective mixing and the spring bloom of phytoplankton. *Deep-Sea Res.* 40(JGOFS special issue):389–408.
- Tett, P. (1990) The photic zone. In: *Light and Life in the Sea*. P. J. Herring, A.K. Campbell, M. Whitfield and L. Maddock (eds). Cambridge: Cambridge Univ. Press, pp. 59–97.
- Tett, P., and Edwards, A. (1984) Mixing and plankton: an interdisciplinary theme in oceanography. *Oceanogr. Mar. Biol. Ann. Rev.*, 22:99–123.
- Valiela, I. (1991) Ecology of water columns. In: *Fundamentals of Aquatic Ecology*. R.S.K. Barnes and K.H. Mann (eds). Oxford: Blackwell Scientific Publications, pp. 29–56.
- Wolf, U., and Woods, J.D. (1988) Lagrangian simulation of primary production in the physical environment – the deep chlorophyll maximum and nutricline. In: *Towards a Theory on Biological-Physical Interactions in the World Ocean*. B. J. Rothschild (ed.). Dordrecht: Kluwer, pp. 51–70.
- Woods, J.D. (1968) Wave-induced shear instability in the summer thermocline. *J. Fluid Mech.* 32:791.
- Woods, J.D. (1980) Diurnal and seasonal variation of convection in the wind-mixed layer of the ocean. *Q. J. R. Meteor. Soc.* 106:379–394.
- Woods, J.D., and Barkmann, W. (1986) The influence of solar heating on the upper ocean. I. The mixed layer. *Q. J. R. Meteor. Soc.* 112:1–27.
- Woods, J.D., and Barkmann, W. (1993) The plankton multiplier – positive feedback in the greenhouse. *J. Plankton Res.* 15(9):1053–1074.
- Woods, J.D., and Onken, R. (1982) Diurnal variation and primary production in the ocean – preliminary results of a Lagrangian ensemble model. *J. Plankton Res.* 4:735–756.
- Yamakazaki, H., and Osborn, T.R. (1988) Review of oceanic turbulence: implications for biodynamics. In: *Towards a Theory on Biological-Physical Interactions in the World Ocean*. B. J. Rothschild (ed.). Dordrecht: Kluwer, pp. 215–234.

APPENDIX

The one-dimensional ecology model includes a phytoplankton model, which is based on a quota method for growth and reproduction, a model of vertical migration and growth of herbivorous zooplankton, a carbon model and a physical upper ocean mixed layer model forced by surface buoyancy fluxes. Section 1 describes the equations and parameters used in the biological model. In section 2, the equations used in the carbon model are presented.

1. Biological model

A. Phytoplankton: cells

The variables of state for each phytoplankton cell are:

1. depth: z
2. light adaptation: I_m
3. internal nitrogen pool: N_p
4. internal energy pool: E_p

Phytoplankton growth depends on the change in nutrients and energy in each plant. The governing equations are:

Uptake of nitrate $N(z)$ and ammonium $A(z)$

$$\frac{\partial N_p}{\partial t} = U_{\max} \frac{N(z)}{N(z) + k_N} + u_{\max} \frac{A(z)}{A(z) + k_A}$$

$$U_{\max} = u_{\max} = 4 \times 10^{-10} \text{ mmol N h}^{-1}$$

$$k_N = k_A = 0.5 \text{ mmol m}^{-3}$$

Photosynthesis and light adaptation

$$\frac{\partial E_p}{\partial t} = E_{\text{abs}} - R_p$$

$$E_{\text{abs}} = k_F A I(z) e^{-I I_m}, \quad \frac{\partial I_m}{\partial t} = \frac{I(z) - I_m}{t_a}$$

where A is plankton cross section area πr^2 ; radius $r = 10 \mu\text{m}$; $I(z)$ is irradiance; phytoplankton adaptation time $t_a = 8 \text{ h}$; absorption parameter $k_F = 0.42$; R_p denotes respiration (see below).

Respiration

$$R_p = k_p \frac{B}{B + k_r} W(T)$$

$$W(T) = 0.3 + 0.7T/T_r,$$

where the respiration parameter $k_p = 0.2 \mu \text{ J h}^{-1}$ and T_r is a reference temperature.

The phytoplankton cells are randomly distributed within the mixed layer. A sinking velocity of 1 m d^{-1} is applied in the diurnal and seasonal thermocline.

B. Phytoplankton: particles

In the Lagrangian ensemble method the cells are bundled into particles which move through the water like individual plankters. Every organism in a particle has the same adaptive state. The number of organisms per particle are modified by reproduction, mortality and grazing.

The variable of state is number of cells: n_p .

Reproduction

Reproduction (cell division) occurs when the energy and nutrient pools both exceed their respective values (E_c , N_c). The number of cells are doubled and half the excess energy and nitrogen are transferred to the internal pools of the new cells.

$$\Delta n_p = n_p [1 - N_c \delta(N_p)] [1 - E_c \delta(E_p)],$$

where

$$\delta(a) = \lim_{b \rightarrow 0} F(a, b):$$

$$F(a, b) = \frac{1}{b} \text{ for } 0 < a < b \text{ else } F(a, b) = 0$$

and $a = N_p$, $b = N_c$.

$$N_{p(\text{new})} = 0.5(N_{p(\text{old})} - N_c), \quad E_{p(\text{new})} = 0.5(E_{p(\text{old})} - E_c)$$

$$E_c = 0.14 \text{ mJ}, \quad N_c = 4 \text{ pmol N}$$

Mortality

Phytoplankton mortality depends on the change in the energy pool due to respiration. A steadily sinking cell loses energy until the energy pool is empty. At this stage, the organism is declared to be dead and will be treated as detritus.

Grazing

The amount of phytoplankton biomass reduced by grazing in each 1 m depth interval is recalculated into the equivalent number of cells. Then the organisms in each particle within the 1 m depth interval are reduced by the corresponding percentage of the lost biomass.

$$\frac{\partial n_p}{\partial t} = -n_p \frac{\Sigma I_g}{P(z)},$$

where ΣI_g represents the phytoplankton biomass loss and $P(z)$ is the phytoplankton biomass per depth interval.

C. Herbivorous zooplankton: individuals

The variables of state for each herbivore are:

1. depth z
2. state of satiation: S

3. weight: G

4. age: A

Zooplankton growth and reproduction depends on the ingestion of phytoplankton biomass. The vertical migration is controlled by the visible light and the food supply. The governing equations are:

Ingestion

$$I_g = \frac{W(T,G)}{|z_2 - z_1|} \int_{z_1}^{z_2} FP^*(z) \frac{P^*(z)}{P^*(z) + k_I} dz$$

$$|z_2 - z_1| = |V_m| dt,$$

where V_m is vertical migration velocity,

$$P^*(z) = P(z) - P_m, \quad 0 < I_g < I_{gmax}$$

$$\text{and } W(T,G) = \left[0.3 + 0.7 \frac{T(z)}{T_r} \right] \frac{G_{eff}^{0.7}}{G_{max}^{0.7}}$$

$$I_{gmax} = 0.84 \text{ cells s}^{-1} - 0.64 \text{ cells s}^{-1} S(t)$$

where filtration rate $F = 1.0 \times 10^{-9} \text{ m}^3 \text{ s}^{-1}$; $P(z)$ is phytoplankton concentration (cells m^{-3}); the minimum concentration for grazing $P_m = 10^5 \text{ cells m}^{-3}$; and the half saturation parameter $k_I = 4.0 \times 10^6 \text{ cells m}^{-3}$.

Growth

$$\frac{\partial G}{\partial t} = k_a I_g c - R_s k_a I_g c - R_b G_{max}^{0.7} [W(T,G) + k_p],$$

where I_g is ingestion; k_a is the assimilation rate; and c is the carbon content of one phytoplankton cell (460 μgC). The metabolic rates are: (a) rate proportional to the food assimilated: $R_s k_a I_g c$, and (b) basal rate: $R_b W(T,G) G_{max}^{0.7}$, where $R_b = 0.3 \times 10^{-3} \text{ h}^{-1}$.

$$k_a(1 - R_s) = 0.7$$

$0.3cI_g$ represents the faecal pellet biomass.

The 'background' respiration is $R_b k_b G_{max}^{0.7}$, where $k_b = 0.1$; maximum weight $G_{max} = 100 \mu\text{gC}$; effective weight $G_{eff} \leq G_{max}$; and the reference temperature $T_r = 10^\circ\text{C}$.

When the total respiration exceeds the actual weight G , the animal is declared dead.

Vertical migration

$$V_m = k_v V_{max} W(T,G)$$

$$k_v = \text{MIN}[k, \text{sign}(1, k)]; \quad \text{for } I_0 = 0$$

$$\text{and } \frac{\partial S}{\partial t} < 0: \quad k_v = -k_v \quad k = 0.4[I(z) - I_r(2 - S)],$$

$$\text{sign}(a,b) = |a| \quad \text{for } b \geq 0, \quad \text{or } -|a| \quad \text{for } b < 0$$

where maximum speed V_{max} is 45 mh^{-1} ; reference radiation $I_r = 1 \text{ Wm}^{-2}$; and I_0 is the surface irradiance.

Thermocline migration:

During daytime the herbivores follow a target isolume $I_r(2 - S)$:

(a) $I(z) > I_r(2 - S)$: $k_v > 0 \rightarrow V_m$ positive (downward motion)

(b) $I(z) < I_r(2 - S)$: $k_v < 0 \rightarrow V_m$ negative (upward motion)

At night, the vertical migration is controlled by the rate of change of satiation:

$$(a) \frac{\partial S}{\partial t} \geq 0: \quad k_v < 0 \rightarrow V_m \text{ negative}$$

$$(b) \frac{\partial S}{\partial t} \leq 0: \quad k_v < 0 \rightarrow V_m \text{ positive}$$

Mixed layer:

The zooplankters are randomly distributed within the mixed layer. During daytime, the additional vertical displacement $V_m \delta t$ is added.

Satiation

$$\frac{\partial S}{\partial t} = \frac{1}{t_m} [I_g / I_{gmax} - S],$$

where relaxation time $t_m = 4 \text{ h}$.

D. Herbivorous zooplankton: particles

The number of individual plankters per particle are modified by reproduction, predation and by starvation. Reproduction takes place 20 d after the animals have reached their maximum weight. After the eggs are hatched, the number of adults decreases over the next 20 d. The transition from a juvenile to an adult zooplankter takes place when G_{max} is exceeded.

The variable of state is the number of individuals: n , n^j = juveniles, n^a is adults, and $n = n^j + n^a$.

Reproduction

$$n^j = k_c n^a \frac{G - G_{min}}{G_{min}}, \quad G^j = G_{min}, \quad G^a = G_{max}$$

where reproduction efficiency $k_c = 0.1$ and $G_{min} = 0.2 \mu\text{gC}$.

Mortality

Mortality after reproduction:

$$\frac{\partial n^a}{\partial t} = \frac{n^a}{-t_w + \int_t^t dt}, \quad \text{for } \int dt \leq t_w - 1^h$$

where $t_w = 20$ d.

Predation:

$$\frac{\partial n}{\partial t} = -nG_{eff}^{0.7}k_{pr} \frac{B}{B + k_B} I(z),$$

where $k_{pr} = 0.6 \times 10^{-4} \text{ d}^{-1}$; B is the total zooplankton biomass; and $k_B = 12\,000 \mu\text{gCm}^{-2}$.

E. Remineralization

Detritus, faecal pellets and the dead animals are bundled into a number of separate particles. The biomass of the particles decays owing to the action of bacteria, following a simple 'radioactive decay' law.

$$\frac{\partial A}{\partial t} = -\frac{\partial C}{\partial t} = aC,$$

where C is the biomass of the dead material and $a = 0.01 \text{ d}^{-1}$.

Other ammonium sources are: predation, reproduction mortality $0.9n^a(G - G_{max})$ and the basal zooplankton respiration rate.

No vertical transfer of nitrate from below the seasonal boundary layer has been taken into account.

2. Carbon model

The chemical cycle of CO_2 in the ocean is governed by a series of equilibria:

1. The CO_2 in the atmosphere equilibrates with seawater via exchange across the air/sea interface



2. The dissolved CO_2 then becomes hydrated



3. The carbonic acid undergoes very rapid dissociation



4. and



H^+ : hydrogen ion concentration

Because the dissociation of carbonic acid to bicarbonate ion is a very fast process, it may for all practical purposes be considered as instantaneous.

The corresponding equilibrium constants can be expressed as follows:

$$K_0 = \frac{[\text{CO}_2]}{p}$$

$$K_1 = \frac{[\text{H}^+][\text{HCO}_3^-]}{[\text{CO}_2]}$$

$$K_2 = \frac{[\text{H}^+][\text{CO}_3^{2-}]}{[\text{HCO}_3^-]},$$

where p is the partial pressure of seawater (see below).

In addition, two other important reactions that affect the balance of the carbonate chemistry are:

$$K_b = \frac{[\text{H}^+][\text{BOH}_4^-]}{[\text{B(OH)}_3]}$$

$$K_w = [\text{H}^+][\text{OH}^-].$$

As CO_2 is added to seawater, the total dissolved inorganic carbon

$$\text{TCO}_2 = [\text{CO}_2] + [\text{HCO}_3^-] + [\text{CO}_3^{2-}]$$

increases, but the alkalinity

$$A = [\text{HCO}_3^-] + 2[\text{CO}_3^{2-}] + [\text{B(OH)}_4^-] + [\text{OH}^-] - [\text{H}^+]$$

remains constant.

Photosynthesis and respiration of biological communities change the concentration of dissolved inorganic carbon. Using a constant C/N ratio of 7, the decrease of inorganic carbon can be directly calculated from the phytoplankton uptake of nitrogen. The sources for CO_2 are remineralization and respiration. The surface CO_2 flux is calculated using a constant piston velocity of 4.8 m d^{-1} .

The model calculates the partial pressure of sea water p using the method described by Bacastrow and Bjorkstrom (1981), which requires as input (1) values for the dissociation constants K_0 , K_1 , K_2 , K_b , K_w and (2) values for TCO_2 , boron and alkalinity.

The initial values are:

$$B(\text{OH})_3 = 409 \times 10^{-6} \text{ mol kg}^{-1}$$

$$p = 325.03 \times 10^{-6} \text{ atm}, p_{atm} = 345 \times 10^{-6} \text{ atm}$$

$$\text{TCO}_2 = 2089.13 \times 10^{-6} \text{ mol kg}^{-1}$$

$$A = 2354.61 \times 10^{-6} \text{ Eq kg}^{-1}$$

TCO_2 and alkalinity were calculated by using a pH-value of 8.25.

The boron concentration as well as alkalinity is assumed to remain constant. The dissociation constants are given by Peng *et al.* (1987).